DRAWING AND EXTRUSION OF COMPOSITE SHEETS, WIRES AND TUBES

DAVID DURBAN†

University Engineering Department, Trumpington Street, Cambridge CB2 1PZ, England

Abstract—Some basic steady forming processes, in particular drawing and extrusion, of composite (multilayered) metal sheets, wires and tubes are analyzed within the framework of continuum plasticity. Material behaviour is modelled as rigid/perfectly-plastic and a radial flow pattern is assumed within the working zone. Simplified versions of the respective Nadai–Hill and Shield radial flow solutions are used for the description of the stress field and velocity profile in each phase (layer). The matching requirements along the interfaces between the different layers, together with the friction conditions at the walls and the entry/exit load specification, lead to a system of algebraic equations that admit a simple solution. The main outcome are elegant formulae for the drawing tension, and extrusion pressure, valid for any number of layers. The applicability of the results is restricted to dies of sufficiently small angles, taper and wall friction. Comparison with experimental results for the drawing stress of bimetallic composites shows a nice agreement, within that range of validity.

1. INTRODUCTION

This paper presents a theoretical study of some basic steady forming processes of multi-layered composites. We investigate in particular the drawing and extrusion, or any combination of both, of composite sheets, wires and tubes, through wedge-shaped and conical dies. An early attempt to analyze such problems has been made in [1], via the force-equilibrium approach. Some experimental data for the required drawing tension of bi-metallic tubes has been given recently in [2], together with a comparative study of a few available numerical methods of analysis.

Here we consider these metal forming processes as a problem in continuum plasticity. The theoretical model employed in this study is based on the following assumptions: (a) The material is rigid/perfectly-plastic according to the von-Mises flow rule; (b) The die is sufficiently long and tapered so that a radial flow pattern can be assumed within the working zone; (c) Deviations from the uniform flow pattern, induced by wall friction and interfacial shear, are small. It is noted that equivalent models have been successfully employed in [3–6] for investigating similar steady forming processes of (single phase) rigid/hardening materials.

The analysis centers on the use of consistent approximations derived from the Nadai–Hill[7, 8] and Shield[9] radial flow solutions, for rigid/perfectly-plastic solids, under plane-strain and axially-symmetric conditions, respectively. A key notion in deriving these approximate solutions is that of the non-uniformity, of the flow field, induced by the presence of friction and shear. We show, following [5, 6], how suitable measures of that non-uniformity can be interpreted directly in terms of physical and kinematical quantities associated with the flow field.

The simplified versions of the exact radial flow solutions, which are valid for small deviations from uniformity, are used for simulating the stress field and velocity profile in each phase of the multilayered composite. The unknown integration constants are then determined from the matching (stress continuity) conditions along the interfaces between the different layers, the entry/exit load specification, and the friction conditions along the walls. The latter are imposed in two alternative fashions: either through the friction factors or through the average Coulomb friction coefficients.

The present investigation results in simple and compact expressions for the stress field in each layer. Useful formulae are thus obtained for the drawing tension, and extrusion

†On sabbatical leave (until September 1983). Permanent address: Department of Aeronautical Engineering, Technion-Israel Institute of Technology, Haifa, Israel.

pressure, as a function of die geometry, composite properties and wall friction. These results are valid for any number of layers in both plane-strain and axially-symmetric forming condition.

We begin in the next section with the derivation of the approximate version of the Nadai–Hill solution for plane-strain radial flow. Next, in Section 3, we analyze in detail the forming processes of composite sheets. A further discussion and comparison with experimental results for the drawing of bimetallic composites is presented in Section 4. The agreement with the theoretical predictions is quite good within the range of applicability of our analysis. Then, in Section 5, we turn to the corresponding axially-symmetric problem and derive the approximate version of Shield's three dimensional radial flow solution. That approximation is applied in Section 6 for the analysis of drawing and extrusion of composite tubes and wires. The presentation in Sections 5 and 6 is less elaborated than the analogous discussion of plane strain problems (in Sections 2 and 3), as we take advantage of the similarity between the two cases to shorten the analysis for axially-symmetric problems. Finally, in Section 7, we point out the common structure of the basic formulae for the driving stresses in the plane-strain and axially-symmetric forming processes.

2. THE NADAI-HILL SOLUTION

Consider plane-strain radial flow of a rigid/perfectly plastic material, where all streamlines are directed towards the same virtual apex 0. Locating the origin of a plane polar system (r, θ) at 0 we have, by virtue of material incompressibility, that the radial velocity should be of the form

$$V_r = -\frac{f(\theta)}{\rho} \tag{1}$$

where $f(\theta)$ is a function of θ, and ρ is a suitably nondimensionalized radial coordinate. The components of the Eulerian strain rate tensor are therefore

$$D_r = -D_\theta = \frac{f(\theta)}{\rho^2}, \quad D_{r\theta} = -\frac{f'(\theta)}{2\rho^2} \tag{2}$$

where the prime denotes differentiation with respect to θ.

The constitutive relations for a rigid/perfectly-plastic material, obeying the von-Mises flow rule, can be written as

$$\left(\frac{\sigma_r - \sigma_\theta}{2}\right)^2 + \tau_{r\theta}^2 = \frac{1}{3}Y^2, \quad \frac{2\tau_{r\theta}}{\sigma_r - \sigma_\theta} = -\frac{f'(\theta)}{2f(\theta)} \tag{3}$$

where $(\sigma_r, \sigma_\theta, \tau_{r\theta})$ are the usual polar stress components, and Y denotes the uniaxial yield stress of the material. It is convenient to introduce here a new variable ψ so that

$$\sigma_r - \sigma_\theta = \frac{2Y}{\sqrt{3}}\cos 2\psi, \quad \tau_{r\theta} = \frac{Y}{\sqrt{3}}\sin 2\psi \tag{4}$$

and, by the second of (3),

$$\frac{f'(\theta)}{2f(\theta)} = -\tan 2\psi. \tag{5}$$

Turning to the equilibrium requirements we find that the equilibrium equations are completely satisfied[7, 8] if

$$\theta = \theta_0 - \psi + \frac{c}{\sqrt{c^2 - 1}}\arctan\left[\sqrt{\frac{c+1}{c-1}}\tan \psi\right], \quad c > 1 \tag{6}$$

where θ_0, c are integration constants.

The normal stresses can now be written in the form[7, 8]

$$\sigma_r = -\frac{2Y}{\sqrt{3}} c \ln \rho + \frac{2Y}{\sqrt{3}}\left[\bar{A} + \frac{1}{2}\cos 2\psi - \frac{1}{2}c \ln(c - \cos 2\psi)\right] \tag{7}$$

$$\sigma_\theta = -\frac{2Y}{\sqrt{3}} c \ln \rho + \frac{2Y}{\sqrt{3}}\left[\bar{A} - \frac{1}{2}\cos 2\psi - \frac{1}{2}c \ln(c - \cos 2\psi)\right] \tag{8}$$

where $\bar{A}$ is another integration constant. The shear stress is expressed by the second of (4) and the velocity profile follows from (5), with the aid of (6), as[8]

$$f = \frac{\bar{U}}{c - \cos 2\psi} \tag{9}$$

where $\bar{U}$ is a constant.

We focus now attention on a restricted version of this general solution where the non-uniformity of the flow field is relatively small. To this end we note that in uniform (frictionless) flow $\tau_{r\theta} = 0$ and $\psi = 0$. A reasonable measure of the deviation from that uniform flow pattern will therefore be the local friction factor defined by

$$m = \frac{\sqrt{3}|\tau_{r\theta}|}{Y}, \quad 0 \leqslant m \leqslant 1. \tag{10}$$

It follows, from the second of (4), that $m = |\sin 2\psi|$ or, for small values of the friction factor, $m \approx 2|\psi|$. This suggests that when the non-uniformity, induced by wall friction and interfacial shear, remains small $(m \ll 1)$ we may regard $|\psi|$ as very small and use approximations of the type $\sin 2\psi \approx 2\psi$, $\cos 2\psi \approx 1$, etc. Relation (6) is then replaced by $\psi \approx (c - 1)(\theta - \theta_0)$ and the simplified version of the stress field is readily found as

$$\frac{\sqrt{3}}{2} \sigma_r = Y + A - B \ln \rho \tag{11}$$

$$\frac{\sqrt{3}}{2} \sigma_\theta = A - B \ln \rho \tag{12}$$

$$\frac{\sqrt{3}}{2} \tau_{r\theta} = (B - Y)\theta - K \tag{13}$$

where

$$A = Y\left[\bar{A} - \frac{1}{2} - \frac{1}{2}c \ln(c - 1)\right], \quad B = Yc, \quad K = Y(c - 1)\theta_0. \tag{14}$$

Similarly, the velocity profile (9) becomes, to the first order, a constant

$$f = U \quad \text{where} \quad U = \frac{\bar{U}}{c - 1}. \tag{15}$$

In passing we note a different interpretation for the amount of deviation from uniformity, based on Truesdell's measure of vorticity[10], defined by

$$M = \left(\frac{|\mathbf{W} \cdot\cdot \mathbf{W}|}{\mathbf{D} \cdot\cdot \mathbf{D}}\right)^{1/2} \tag{16}$$

where $\mathbf{D}$ is the Eulerian strain rate tensor and $\mathbf{W}$ is the associated spin tensor. Now, for the radial flow pattern (1) the only nonvanishing component of $\mathbf{W}$ is $W_{r\theta} = -f'(\theta)/2\rho^2$.

Inserting this, together with (2), in definition (16), and observing (5), gives

$$M = |\sin 2\psi|. \tag{17}$$

In uniform flow $M = 0$, and for nearly uniform flows we may argue, on a purely kinematical basis, that M remains very small. This implies again, via (17), that $|\psi|$ is small, thus providing a kinematical justification for approximations (11)–(15). Of course, for the particular radial flow pattern (1) we have that $m = M$.

3. COMPOSITE SHEETS

Figure 1 illustrates a steady forming process where the dimensions of a composite multilayered sheet are reduced by drawing (or extruding) it through a wedge-shaped die. The composite consists of n layers ($i = 1, 2, \ldots, n$) and its initial thickness H is reduced, during the forming process, to the final thickness h. The entry to and exit from the die are modelled by the arcs $\rho = \rho_0$ and $\rho = 1$, respectively. We assume also that the die is sufficiently long and tapered so as to permit the use of averaged boundary conditions at the entry and exit. Within the working zone we assume a radial flow pattern where the streamlines of all layers are directed towards the common apex 0. Each layer is modelled as rigid/perfectly-plastic and deviations from uniformity, induced by wall friction and by interfacial shear, are assumed to be small. Under these conditions we may use relations (11)–(13) for the description of the stress field in each layer. Thus

$$\frac{\sqrt{3}}{2}\sigma_r^{(i)} = Y_i + A_i - B_i \ln \rho \tag{18}$$

$$\frac{\sqrt{3}}{2}\sigma_\theta^{(i)} = A_i - B_i \ln \rho \tag{19}$$

$$\frac{\sqrt{3}}{2}\tau_{r\theta}^{(i)} = (B_i - Y_i)\theta - K_i \tag{20}$$

where $i = 1, 2, \ldots, n$; Y_i is the yield stress of layer "i" and $\alpha_{i-1} \leqslant \theta \leqslant \alpha_i$ (note that for the sake of consistency the α_i are taken as negative if they fall in the negative range of θ). Similarly, the velocity profile within each layer, as obtained from (1) and (15), is simply

$$V_r^{(i)} = -\frac{U_i}{\rho} \quad i = 1, 2, \ldots, n. \tag{21}$$

On the whole we have therefore $4n$ unknowns, A_i, B_i, K_i, U_i $i = 1, 2, \ldots, n$, that should be determined from an equal number of boundary conditions.

The kinematical conditions of velocity continuity may be separated from the stress
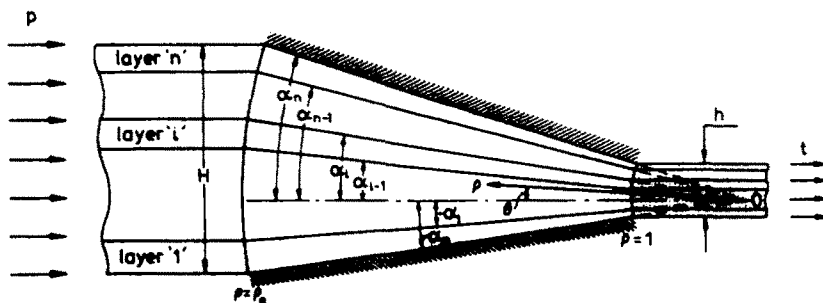

Fig. 1. Notation for composite multilayered sheet drawing or extrusion. The sheet enters the working zone, at $\rho = \rho_0$, with initial thickness H and leaves the die, at $\rho = 1$, with the reduced thickness h. The reduction is defined as $R = 1 - h/H = 1 - 1/\rho_0$. The composite consists of n layers ($i = 1, 2, \ldots, n$) and all streamlines are radially directed towards the same virtual apex 0.

conditions, viz.

$$U_i = U_{i+1} \quad i = 1, 2, \ldots, n - 1. \tag{22}$$

The solution of (22) is $U_i = U$ ($i = 1, 2, \ldots, n$) where constant U is left undetermined. The radial velocity profile remains therefore (within the present approximation) constant over any arc $\rho = \text{constant}$, regardless of the number and arrangement of layers.

Continuity of normal stress σ_θ at the interfaces requires, via (19), that

$$A_i = A_{i+1}, \quad B_i = B_{i+1} \quad i = 1, 2, \ldots, n - 1. \tag{23}$$

It follows that all constants A_i are equal and that all constants B_i are equal, namely

$$A_i = A, \quad B_i = B \quad i = 1, 2, \ldots, n \tag{24}$$

where A, B are as yet unknown. Relations (24) imply that the circumferential stress (19) is the same for all layers. Continuity of shear stress (20) along the interfaces requires that

$$K_{i+1} - K_i + (Y_{i+1} - Y_i)\alpha_i = 0 \quad i = 1, 2, \ldots, n - 1. \tag{25}$$

where we have used the second of (24). By now we have been left with $n + 2$ unknowns: K_i ($i = 1, 2, \ldots, n$), A and B. Thus, three additional conditions are required so as to form together with (25) the desired number of equations.

Two equations are supplied by the friction condition along the walls $\theta = \alpha_0$ and $\theta = \alpha_n$. These conditions however may be stated in two different ways. One possibility is to impose the respective shear factors (m_0, m_n) along the walls. This leads, by (10) and (20), to the equations

$$(B - Y_1)\alpha_0 - K_1 = -\frac{1}{2} m_0 Y_1 \tag{26}$$

$$(B - Y_n)\alpha_n - K_n = \frac{1}{2} m_n Y_n. \tag{27}$$

Note that along the walls the shear stress opposes the flow and should therefore be taken as positive at $\theta = \alpha_n$, but as negative at $\theta = \alpha_0$.

Alternatively, we can implement the friction boundary data by imposing the average Coulomb friction coefficients (μ_0, μ_n) through the integral conditions

$$\int_1^{\rho_0} \tau_{r\theta}^{(1)} \, d\rho = \mu_0 \int_1^{\rho_0} \sigma_\theta \, d\rho \qquad \text{at } \theta = \alpha_0 \tag{28}$$

$$\int_1^{\rho_0} \tau_{r\theta}^{(n)} \, d\rho = -\mu_n \int_1^{\rho_0} \sigma_\theta \, d\rho \quad \text{at } \theta = \alpha_n \tag{29}$$

(σ_θ is expected to be negative). Inserting (19) and (20) in (28) and (29) and observing (24) gives the equations

$$(B - Y_1)\alpha_0 - K_1 = \mu_0(A - JB) \tag{30}$$

$$(B - Y_n)\alpha_n - K_n = -\mu_n(A - JB) \tag{31}$$

where

$$J = \frac{\rho_0 \ln \rho_0}{\rho_0 - 1} - 1. \tag{32}$$

Finally, we have the loading condition which determines the ratio between the average drawing tension at the exit and the average extrusion pressure at the entry. We assume that the die angle $(\alpha_n - \alpha_0)$ is sufficiently small (which is indeed the common case in practice) to permit replacement of horizontal drawing and extrusion stresses by the corresponding radial stress components. Accordingly, we define the average drawing tension stress t, and average extrusion pressure p, as

$$t = \frac{1}{\alpha_n - \alpha_0} \int_{\alpha_0}^{\alpha_n} \sigma_r(\rho = 1)\, \mathrm{d}\theta, \quad p = -\frac{1}{\alpha_n - \alpha_0} \int_{\alpha_0}^{\alpha_n} \sigma_r(\rho = \rho_0)\, \mathrm{d}\theta. \tag{33}$$

The loading condition is now stated in the form

$$(1 - \eta)t - (1 + \eta)p = 0 \tag{34}$$

where the specified loading parameter η describes the type of the forming process. Thus $\eta = 1$ in pure drawing $(p = 0)$, $\eta = -1$ in pure extrusion $(t = 0)$, and $\eta > 1$ describes drawing with back-pull $(p < 0)$. Inserting σ_r from (18) in definitions (33), and noting (24), we get

$$t = \frac{2}{\sqrt{3}}(Y_{av} + A), \quad p = -\frac{2}{\sqrt{3}}(Y_{av} + A - B \ln \rho_0) \tag{35}$$

where Y_{av} is the average yield stress of the composite defined by

$$Y_{av} = \frac{1}{\alpha_n - \alpha_0} \sum_{i=1}^{n} (\alpha_i - \alpha_{i-1}) Y_i \tag{36}$$

The loading condition (34) can now be written, with the aid of (35), in the form

$$A - \frac{1 + \eta}{2}(\ln \rho_0)B + Y_{av} = 0. \tag{37}$$

To summarize then, the governing set of equations, for the $n + 2$ integration constants $(K_i\ i = 1, 2, \ldots, n, A, B)$ consists of the $n - 1$ equations given by (25), the two friction conditions (26) and (27), or (30) and (31), and the loading condition (37). The solution of this system is readily obtained in the following way: Summing eqns (25), from $i = 1$ to $i = n - 1$, gives

$$K_n - K_1 + \alpha_n Y_n - \alpha_0 Y_1 - (\alpha_n - \alpha_0)Y_{av} = 0. \tag{38}$$

Now, eqn (38) together with (26) and (27), or (30) and (31), and (37) are easily solved for A, B, K_1, K_n. When the friction factor is imposed along the walls, (26) and (27), we get

$$A = \left[(1 + \delta)\left(\frac{1 + \eta}{2} \ln \rho_0\right) - 1\right] Y_{av}, \quad B = (1 + \delta)Y_{av} \tag{39}$$

$$K_1 = \alpha_0(Y_{av} - Y_1) + \gamma Y_{av}, \quad K_n = \alpha_n(Y_{av} - Y_n) + \gamma Y_{av} \tag{40}$$

where

$$\delta = \frac{m_n Y_n + m_0 Y_1}{2(\alpha_n - \alpha_0)Y_{av}} \tag{41}$$

$$\gamma = \frac{\alpha_0 m_n Y_n + \alpha_n m_0 Y_1}{2(\alpha_n - \alpha_0)Y_{av}}. \tag{42}$$

Relations (39) and (40) represent also the solution for the case where the Coulomb friction

coefficient is imposed along the walls, (30) and (31), only that (41) and (42) are then replaced by

$$\delta = \frac{(\mu_n + \mu_0)\left(1 - \frac{1+\eta}{2} \ln \rho_0 + J\right)}{(\alpha_n - \alpha_0) + (\mu_n + \mu_0)\left(\frac{1+\eta}{2} \ln \rho_0 - J\right)} \tag{43}$$

$$\gamma = \frac{(\alpha_0 \mu_n + \alpha_n \mu_0)\left(1 - \frac{1+\eta}{2} \ln \rho_0 + J\right)}{(\alpha_n - \alpha_0) + (\mu_n + \mu_0)\left(\frac{1+\eta}{2} \ln \rho_0 - J\right)}. \tag{44}$$

The remaining constants K_i $(i = 2, 3, \ldots, n - 1)$ are easily obtained from eqns (25). Summing the first $i - 1$ equations, and arranging, gives

$$K_i - K_1 + \alpha_i Y_i - \alpha_0 Y_1 - (\alpha_i - \alpha_0) Y_{av}^{(i)} = 0 \tag{45}$$

where $Y_{av}^{(i)}$ is the average yield stress of the first i layers, viz

$$Y_{av}^{(i)} = \frac{1}{\alpha_i - \alpha_0} \sum_{j=1}^{i} (\alpha_j - \alpha_{j-1}) Y_j. \tag{46}$$

Note that $Y_{av}^{(1)} = Y_1$ and $Y_{av}^{(n)} = Y_{av}$. Combining the first of (40) with (45) we find that

$$K_i = \alpha_0 (Y_{av} - Y_{av}^{(i)}) + \alpha_i (Y_{av}^{(i)} - Y_i) + \gamma Y_{av} \tag{47}$$

which completes the solution. The formula for K_i can be written in a number of different forms but here we prefer to use (47). It may be verified that expression (47) agrees with relations (40) when $i = 1$ and $i = n$, respectively.

The stress field within the deformation zone follows now from (18)–(20), with the aid of (39) and (47), as

$$\frac{\sqrt{3}}{2} \sigma_r^{(i)} = Y_i - Y_{av} + (1 + \delta) Y_{av} \left(\frac{1+\eta}{2} \ln \rho_0 - \ln \rho\right) \tag{48}$$

$$\frac{\sqrt{3}}{2} \sigma_\theta = -Y_{av} + (1 + \delta) Y_{av} \left(\frac{1+\eta}{2} \ln \rho_0 - \ln \rho\right) \tag{49}$$

$$\frac{\sqrt{3}}{2} \tau_{r\theta}^{(i)} = [(1 + \delta)\theta - \alpha_0 - \gamma] Y_{av} - (\alpha_i - \alpha_0) Y_{av}^{(i)} + (\alpha_i - \theta) Y_i \tag{50}$$

and the corresponding drawing tension and extrusion pressure, (35), become

$$t = \frac{2}{\sqrt{3}} (1 + \delta) \left(\frac{1+\eta}{2} \ln \rho_0\right) Y_{av}, \quad p = \frac{2}{\sqrt{3}} (1 + \delta) \left(\frac{1-\eta}{2} \ln \rho_0\right) Y_{av}. \tag{51}$$

A helpful notion here is that of the uniform drawing tension (t_u) and uniform extrusion pressure (p_u), which are the required driving stresses when the walls are smooth. In the absence of wall friction we have that $\delta = 0$, and so

$$t_u = \frac{1+\eta}{\sqrt{3}} Y_{av} \ln \rho_0, \quad p_u = \frac{1-\eta}{\sqrt{3}} Y_{av} \ln \rho_0. \tag{52}$$

The driving stresses (51) can now be rewritten in the form

$$t = (1 + \delta)t_u, \quad p = (1 + \delta)p_u \tag{53}$$

emphasizing thus the role of δ as a correction factor which depends on the details of friction data along the walls.

4. DISCUSSION OF THE PLANE-STRAIN SOLUTION

We have already seen how the effects of wall friction can be implemented either through the friction factors or through the Coulomb friction coefficients. There are however additional noticeable differences between the results obtained by these two approaches to the friction conditions.

Relation (41) suggests a dependence of the correction factor δ on material properties; it appears that the use of soft coating layers will reduce the required driving stress. Consider for example a symmetric composite where a hard core is coated with thin soft layers. Put $m_0 = m_n = m$ for the shear factor, $\alpha_n - \alpha_0 = \alpha$ for the die angle, $Y_1 = Y_n = Y_{coat}$ for the yield stress of the coating material, and identify Y_{av} with the core material yield stress Y_{core} (this is permissible for a sufficiently thin coating material). Relation (41) is then reduced to

$$\delta = \left(\frac{m}{\alpha}\right)\left(\frac{Y_{coat}}{Y_{core}}\right) \tag{54}$$

predicting a relatively small δ for law values of Y_{coat}/Y_{core}. This behaviour was observed in experiments reported in [11].

By contrast, relation (43) is independent of material properties, but does depend quite strongly on the reduction and loading parameter. In pure drawing, with $\eta = 1$, we have

$$\delta = \frac{q\left(\dfrac{\ln \rho_0}{\rho_0 - 1}\right)}{1 + q\left(1 - \dfrac{\ln \rho_0}{\rho_0 - 1}\right)} \quad \text{with} \quad q = \frac{\mu_n + \mu_0}{\alpha_n - \alpha_0} \tag{55}$$

while in pure extrusion, where $\eta = -1$,

$$\delta = \frac{q\left(\dfrac{\rho_0 \ln \rho_0}{\rho_0 - 1}\right)}{1 - q\left(\dfrac{\rho_0 \ln \rho_0}{\rho_0 - 1} - 1\right)}. \tag{56}$$

Relations (55) and (56) are displayed in Fig. 2 over the practical range of parameter q and the effective homogeneous strain ϵ_0 given by

$$\epsilon_0 = \frac{2}{\sqrt{3}} \ln \rho_0. \tag{57}$$

It is seen from Fig. 2 that the correction factor in pure extrusion is higher than that in pure drawing. This implies, via (53), that for the same friction coefficients and die geometry the required extrusion pressure is higher than the corresponding drawing tension. That result is not altogether unexpected as the extrusion pressure causes lateral expansion of the sheet, thus increasing the pressure on the walls which in turn increases the resisting shear stresses. By contrast, the lateral contraction caused by the drawing tension has an opposite effect on the shear stresses along the walls. For small q and ϵ_0 we can replace (43)
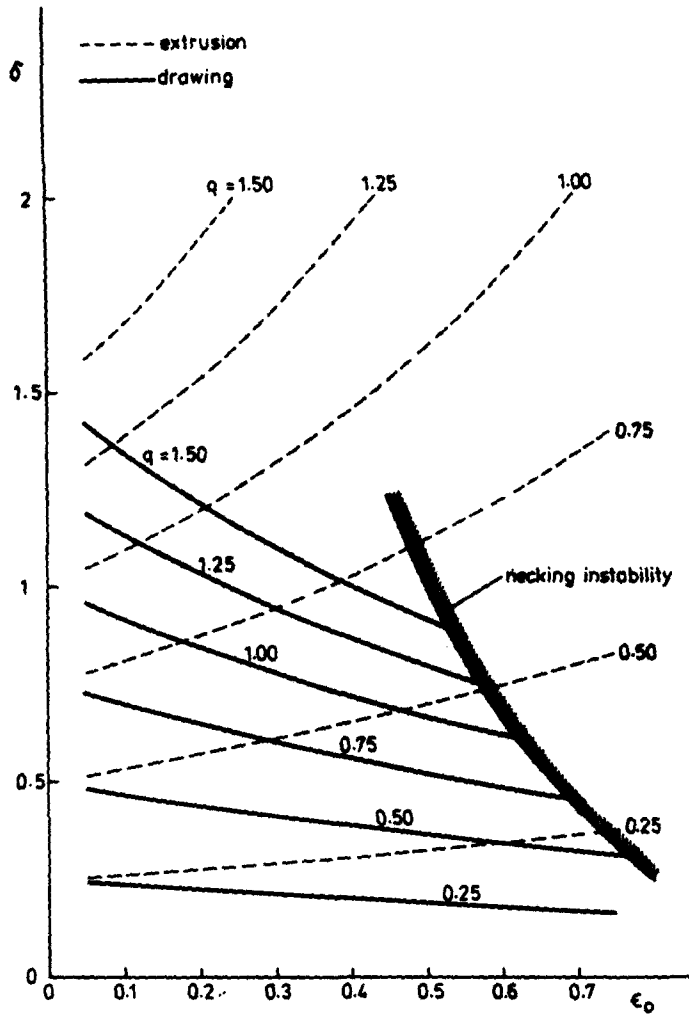
Fig. 2. Variation of the correction factor δ with the effective homogeneous strain $\epsilon_0 = (2/\sqrt{3}) \ln \rho_0$, for different values of parameter $q = (\mu_n + \mu_0)/(\alpha_n - \alpha_0)$, in pure drawing and pure extrusion. Calculations are based on Coulomb's friction conditions.

by the approximation

$$\delta \approx q \left[1 - \frac{\sqrt{3}}{4} (1 + q) \eta \epsilon_0 \right] \tag{58}$$

revealing, to this degree of accuracy, a linear dependence on $\eta \epsilon_0$.

It is difficult to tell which of the two alternative friction conditions, imposed along the walls, is closer to reality. There is a definite possibility that the actual friction data, associated with large plastic deformations, is some combination of the alternatives considered here. That idea will not be explored any further in this paper, and we shall just point out that for sufficiently small values of q and ϵ_0 relations (43) and (44) become identical with (41)–(42), when m_i is linearly related to μ_i, viz

$$\frac{1}{2} m_i \frac{Y_i}{Y_{av}} = \mu_i \left(1 - \frac{\sqrt{3}}{4} \eta \epsilon_0 \right) \quad i = 0, n. \tag{59}$$

Of course, the accuracy of our model becomes questionable when δ increases. The local shear factor (10), which according to our basic assumption should remain much smaller

than unity, follows from (50) as

$$m^{(i)} = 2 \left| [(1 + \delta)\theta - \alpha_0 - \gamma] \frac{Y_{av}}{Y_i} - (\alpha_i - \alpha_0) \frac{Y_{av}^{(i)}}{Y_i} + (\alpha_i - \theta) \right| \tag{60}$$

$$\alpha_{i-1} \leqslant \theta \leqslant \alpha_i, \quad i = 1, 2, \ldots, n.$$

The linear dependence of $m^{(i)}$ on θ within each layer implies that the highest values of the friction factor are attained at the interfaces. A typical interface value m_i is obtained from (60), with $\theta = \alpha_i$, as

$$m_i = 2 \left| (\alpha_i - \alpha_0) \frac{Y_{av} - Y_{av}^{(i)}}{Y_i} + (\alpha_i \delta - \gamma) \frac{Y_{av}}{Y_i} \right| \quad i = 1, 2, \ldots, n - 1. \tag{61}$$

For small die angles we may expect m_i to remain within the range of validity of our analysis, provided that δ is not too high. The presence of soft layers with yield stresses which are considerably below Y_{av} will obviously increase the values of m_i. A more accurate analysis, based on the complete solution (6) is then required.

There are additional limits on the validity of the present model which will be mentioned briefly. In the first place it is required that the die will have a sufficiently small taper to justify the radial flow assumption. This requirement, when expressed in geometrical terms, implies that the die angle $(\alpha_n - \alpha_0)$ should be some fraction of the reduction $R = 1 - 1/\rho_0$. Secondly, the drawing tension cannot exceed the average yield stress Y_{av}. For pure drawing, we can put this condition in the form (see also Fig. 2)

$$(1 + \delta)\epsilon_0 \leqslant 1. \tag{62}$$

It is also possible that the nature of the bond at the interfaces places a restriction on the stress field. Suppose for example that the allowable shear stress at each interface is $\tau_0^{(i)}$. There are then $(n - 1)$ constraints, obtained from (50),

$$\frac{2}{\sqrt{3}} \left| (\alpha_i - \alpha_0)(Y_{av} - Y_{av}^{(i)}) + (\alpha_i \delta - \gamma)Y_{av} \right| \leqslant \tau_0^{(i)} \quad i = 1, 2, \ldots, n - 1 \tag{63}$$

that should be observed.

We turn now to a comparison of theoretical predictions obtained here with the experimental results reported in [2] for pure drawing of bimetallic composites.

The experiments were carried on tubes drawn through conical dies over stationary cylindrical plugs. The stress field in that flow pattern is close to plane-strain conditions with $\alpha_0 = 0$. (The axially-symmetric radial flow solution, discussed in the next sections, is not valid for tubes with $\alpha_0 = 0$.) The composites were made from various combinations of mild steel (MS), 70/30 brass (Br), and pure copper (Cu). The uniaxial stress–strain characteristics of these materials are represented by the power-hardening relation

$$\sigma = Y_0(1 + \zeta\epsilon)^n \tag{64}$$

with the particular specifications: $Y_0 = 451.4 \, \text{MPa}$, $\zeta = 66.7$, $n = 0.151$ for mild steel; $Y_0 = 260.9 \, \text{MPa}$, $\zeta = 38.5$, $n = 0.235$ for 70/30 brass; and $Y_0 = 242.6 \, \text{MPa}$, $\zeta = 45.5$, $n = 0.096$ for pure copper.

The hardening characteristics represented by (64) deviate, as shown in Fig. 3, from the perfectly-plastic behaviour assumed by our model. We define therefore an average yield stress by

$$Y = Y(\epsilon) = \frac{1}{\epsilon} \int_0^\epsilon \sigma \, d\epsilon \tag{65}$$
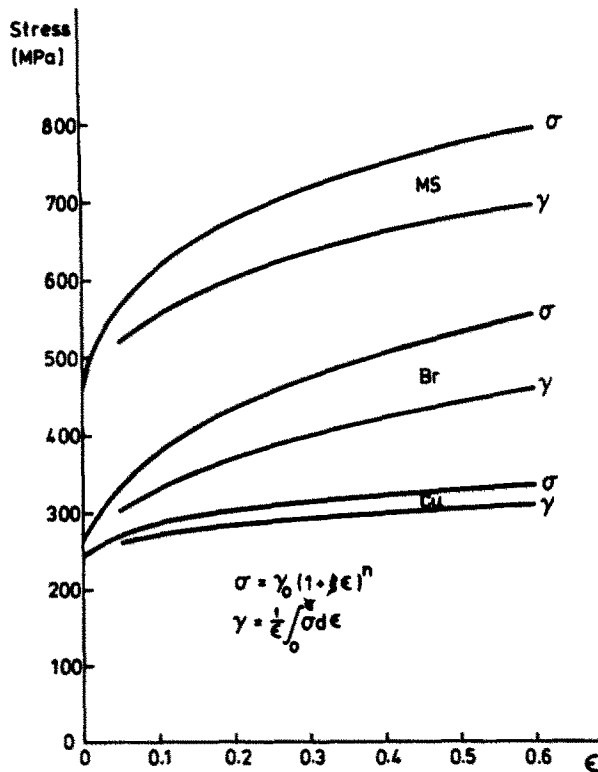
Fig. 3. Uniaxial stress–strain characteristics of three strain-hardening materials. Mild steel (MS): $Y_0 = 451.4$ MPa, $\zeta = 66.7$, $n = 0.151$. 70/30 brass (Br): $Y_0 = 260.9$ MPa, $\zeta = 38.5$, $n = 0.235$. Pure copper (Cu): $Y_0 = 242.6$ MPa, $\zeta = 45.5$, $n = 0.096$. Also shown are the integral average yield stresses $Y = Y(\epsilon)$.

and use this definition as a reasonable equivalent description (see Fig. 3) of material (64), suitable for the present analysis.

The composite specimens were bimetallic each, with the following ordering of layers: MS/Cu, Cu/MS, MS/Br and Br/MS (the notation reads outer layer/inner layer). The corresponding geometrical relations were $\alpha_0 = 0$, $\alpha_1 = 0.059$ rad (also $\alpha_1 = 0.046$ rad for the Cu/MS tubes), and $\alpha_2 = 0.131$ rad. The effective homogeneous strain was varied over a fairly wide range. Some uncertainty about the exact values of the friction factors and friction coefficients is reported in [2], together a recommendation of the commonly used values of $m = 0.06$ and $\mu = 0.04$.

Figures 4(a–c) show the comparison between the experimental results of [2], for pure drawing, and the theoretical predictions of the present study. Note that the average drawing stress (52) and (53) can be written in the form $t = (1 + \delta)\epsilon_0 Y_{av}$ where, in view of (65), the average yield stress of the composite Y_{av} is a function of the total homogeneous strain ϵ_0. Thus, Y_{av} increases with ϵ_0 according to the relative proportions of the two layers. The theoretical curves in Figs. 4 were calculated with the correction factor (41) and with the recommended values of $m_0 = m_2 = 0.06$ for the friction factors. However, almost identical results (not shown in Figs. 4) were obtained from relation (55) for the correction factor with $\mu_0 = \mu_2 = 0.04$ (which corresponds to $q = 0.61$).

The agreement between theory and experiment, as displayed in Figs. 4, appears to support the validity of the present analysis. The deviations at low values of ϵ_0 are expected since the die cannot be regarded, in that range, as long and tapered. The geometrical restriction on the dimensions of the die ($\alpha_n - \alpha_0 < 1 - 1/\rho_0$) gives approximately $\epsilon_0 < 0.16$, which indeed bounds the domain of agreement, between theory and experiment, in Figs. 4.
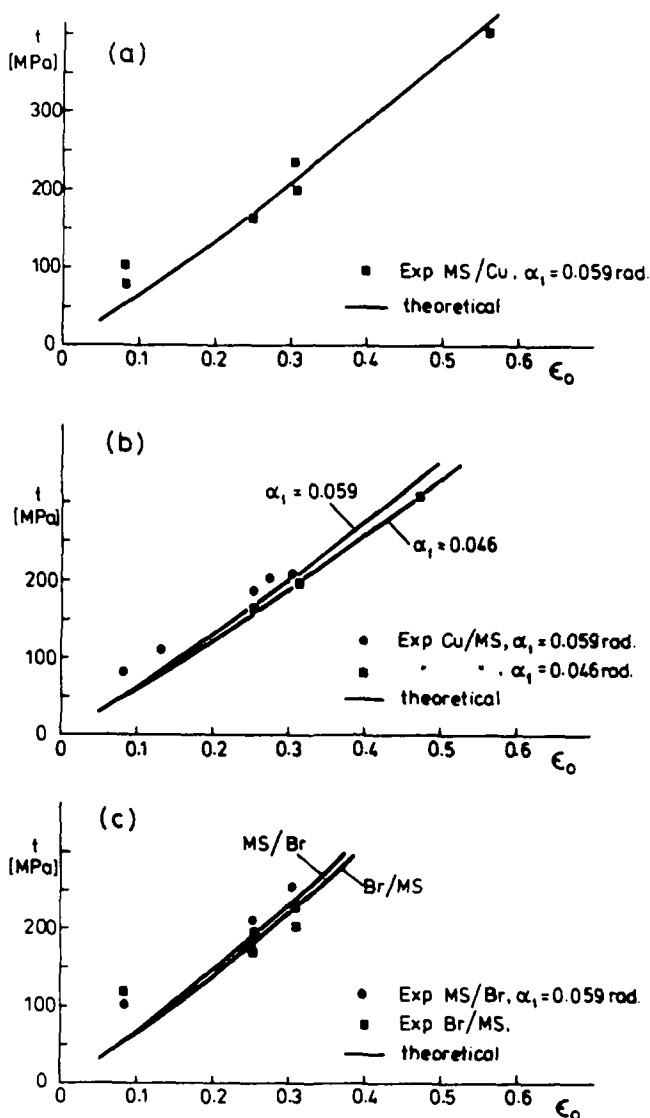
Fig. 4. Comparison of experimental results for the drawing tension t of bimetallic composite tubes with theoretical predictions. The theoretical curves were calculated on the basis of friction factor conditions with $m = 0.06$. In all cases $\alpha_0 = 0$, $\alpha_2 = 0.131$ rad. Theoretical results are expected to be valid for $\zeta_0 < 0.16$.

5. SHIELD'S SOLUTION

Axially-symmetric radial flow is conveniently formulated in a spherical-polar system (r, θ, φ) with the origin at the virtual apex 0. Material incompressibility implies here a radial velocity of the form (ρ-nondimensionalized radial coordinate, $f(\theta)$-unknown function)

$$V_r = -\frac{f(\theta)}{\rho^2}. \tag{66}$$

The components of the Eulerian strain rate follow as

$$D_r = 2\frac{f(\theta)}{\rho^3}, \quad D_\theta = D_\varphi = -\frac{f(\theta)}{\rho^3}, \quad D_{r\theta} = -\frac{f'(\theta)}{2\rho^3}. \tag{67}$$

For a rigid/perfectly-plastic material we have the constitutive relations

$$(\sigma_r - \sigma_\theta)^2 + 3\tau_{r\theta}^2 = Y^2, \quad \frac{3\tau_{r\theta}}{\sigma_r - \sigma_\theta} = -\frac{f'(\theta)}{2f(\theta)}. \tag{68}$$

The first of (68) is identically satisfied with the parametric representation

$$\sigma_r - \sigma_\theta = Y \cos 2\psi, \quad \tau_{r\theta} = \frac{Y}{\sqrt{3}} \sin 2\psi \tag{69}$$

which can be combined with the second of (68) to give

$$\frac{\sqrt{3}f'(\theta)}{6f(\theta)} = -\tan 2\psi. \tag{70}$$

Inserting now (69) in the radial equation of equilibrium and integrating over the streamlines, we find that[9]

$$\sigma_r = -\frac{Y}{\sqrt{3}} [2(\psi' + \sqrt{3}) \cos 2\psi + \cot \theta \sin 2\psi] \ln \rho + \frac{Y}{\sqrt{3}} F(\theta) \tag{71}$$

where $F(\theta)$ is unknown. It can now be shown[9] that transverse equilibrium is satisfied if

$$[2(\psi' + \sqrt{3}) \cos 2\psi + \cot \theta \sin 2\psi]' = 0 \tag{72}$$

$$(F - \sqrt{3} \cos 2\psi)' + 3 \sin 2\psi = 0. \tag{73}$$

Equations (72) and (73) were first derived and solved numerically by Shield[9]. Since they do not admit an exact solution, the approximation procedure will be performed directly on the differential equations.

The local shear factor follows from the second of (69) as

$$m = \frac{\sqrt{3} |\tau_{r\theta}|}{Y} = |\sin 2\psi|. \tag{74}$$

Also, as observed already in [5], the vorticity measure (16) coincides with the local shear factor (74). It follows that, as in the plane-strain problem, we may regard $|\psi|$ as much smaller than unity in nearly uniform radial flow patterns. With this assumption it is permissible to approximate (72) by the equation

$$(\psi' + \sqrt{3}) + \psi \cot \theta = \frac{\sqrt{3}B}{Y} \tag{75}$$

where B is an integration constant. The solution of (75) is conveniently written in the form

$$\psi = \sqrt{3} \left(\frac{B}{Y} - 1\right) \tan \frac{\theta}{2} - \frac{\sqrt{3}K}{2Y \sin \theta} \tag{76}$$

where K is the second integration constant. It is worth mentioning that (76) is also the exact solution[4, 5] for axially-symmetric radial flow of rigid/linear-hardening materials. For small die angles we can replace solution (76) by the relation

$$\frac{2}{\sqrt{3}} \psi = \left(\frac{B}{Y} - 1\right) \theta - \frac{K}{Y\theta}. \tag{77}$$

The corresponding solution of (73), when approximated along similar lines, is simply

$$F = \sqrt{3}\left(1 + \frac{A}{Y}\right) \tag{78}$$

where A is an integration constant.

The stress field follows now as

$$\sigma_r = Y + A - 2B \ln \rho \tag{79}$$

$$\sigma_\theta = A - 2B \ln \rho \tag{80}$$

$$\tau_{r\theta} = (B - Y)\theta - \frac{K}{\theta}. \tag{81}$$

Expressions (79)–(81) may be compared with the analogous results (11)–(13) for the plane-strain problem.

The velocity profile associated with that stress field follows from the solution of (70), with the approximation $\tan 2\psi \approx 2\psi$, and use of (77). The result reads

$$f(\theta) = U\theta^{[(6K)/Y]}\exp\left[-3\left(\frac{B}{Y} - 1\right)\theta^2\right] \tag{82}$$

where U is a constant. For sufficiently small θ we can use a further simplification of (82). Integrating (70) we find that for small ψ and θ

$$f(\theta) = U\exp\left(-4\sqrt{3}\int \psi \, d\theta\right) \approx U \tag{83}$$

6. COMPOSITE TUBES AND WIRES

The basic notation for composite multilayered tube forming processes is shown in Fig. 5. Following the same ideas as in the plane-strain analysis, we assume that eqns (79)–(83) describe the stress field within each layer. Thus

$$\sigma_r^{(i)} = Y_i + A_i - 2B_i \ln \rho \tag{84}$$

$$\sigma_\theta^{(i)} = A_i - 2B_i \ln \rho \tag{85}$$

$$\tau_{r\theta}^{(i)} = (B_i - Y_i)\theta - \frac{K_i}{\theta} \tag{86}$$

where $i = 1, 2, \ldots, n$ and $\alpha_{i-1} \leqslant \theta \leqslant \alpha_i$. The associated radial velocity is obtained from (66)
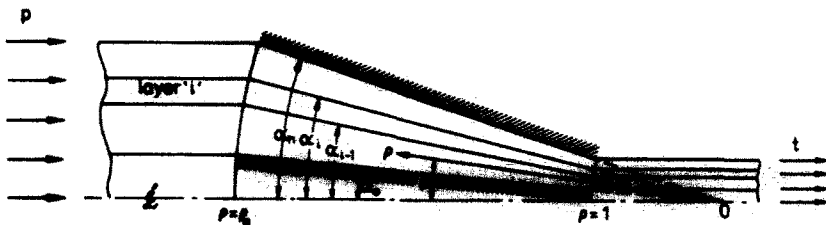

Fig. 5. Notation for composite multilayered tube drawing or extrusion. The tube enters the working zone at $\rho = \rho_0$ and leaves the die, with reduced dimensions, at $\rho = 1$. The composite consists of n layers ($i = 1, 2, \ldots, n$) and all streamlines are directed towards the same virtual apex 0.

and (83) as

$$V_r^{(i)} = -\frac{U_i}{\rho^2} \quad i = 1, 2, \ldots, n. \tag{87}$$

Normal stress continuity at the interfaces is satisfied if

$$A_i = A \quad \text{and} \quad B_i = B \quad i = 1, 2, \ldots, n. \tag{88}$$

The requirement for continuity of shear stresses along the interfaces leads here to the $(n - 1)$ equations

$$K_{i+1} - K_i + (Y_{i+1} - Y_i)\alpha_i^2 = 0 \quad i = 1, 2, \ldots, n - 1. \tag{89}$$

Turning to the friction conditions imposed at the walls, we have either the friction factor version ($m = m_0$ at $\theta = \alpha_0$, $m = m_n$ at $\theta = \alpha_n$)

$$(B - Y_1)\alpha_0^2 - K_1 = -\frac{\alpha_0}{\sqrt{3}} m_0 Y_1 \tag{90}$$

$$(B - Y_n)\alpha_n^2 - K_n = \frac{\alpha_n}{\sqrt{3}} m_n Y_n \tag{91}$$

or the Coulomb friction coefficient version

$$\int_1^{\rho_0} \tau_{r\theta}^{(1)} \rho \, d\rho = \mu_0 \int_1^{\rho_0} \sigma_\theta \rho \, d\rho \qquad \text{at } \theta = \alpha_0 \tag{92}$$

$$\int_1^{\rho_0} \tau_{r\theta}^{(n)} \rho \, d\rho = -\mu_n \int_1^{\rho_0} \sigma_\theta \rho \, d\rho \quad \text{at } \theta = \alpha_n. \tag{93}$$

Substituting the stresses (85) and (86) in conditions (92) and (93) gives the equations

$$(B - Y_1)\alpha_0^2 - K_1 = \alpha_0 \mu_0 (A - JB) \tag{94}$$

$$(B - Y_n)\alpha_n^2 - K_n = -\alpha_n \mu_n (A - JB) \tag{95}$$

where

$$J = \frac{2\rho_0^2 \ln \rho_0}{\rho_0^2 - 1} - 1. \tag{96}$$

The loading condition is again expressed by relation (34) with

$$t = \frac{1}{\alpha_n^2 - \alpha_0^2} \int_{\alpha_0}^{\alpha_n} \sigma_r(\rho = 1)\theta \, d\theta = Y_{av} + A \tag{97}$$

$$p = -\frac{1}{\alpha_n^2 - \alpha_0^2} \int_{\alpha_0}^{\alpha_n} \sigma_r(\rho = \rho_0)\theta \, d\theta = -(Y_{av} + A - 2B \ln \rho_0) \tag{98}$$

as the proper expressions for the driving stresses. The average yield stress of the composite is here defined by

$$Y_{av} = \frac{1}{\alpha_n^2 - \alpha_0^2} \sum_{i=1}^n (\alpha_i^2 - \alpha_{i-1}^2) Y_i. \tag{99}$$

Inserting (97) and (98) in (34) we obtain the axially-symmetric loading condition in the

form

$$A - (1 + \eta)(\ln \rho_0)B + Y_{av} = 0. \tag{100}$$

The solution of equations (89), (100) and (90) and (91), or (94) and (95), is straightforward and follows the procedure employed in the plane-strain analysis. Summing eqns (89) from $i = 1$ to $i = n - 1$ gives

$$K_n - K_1 + \alpha_n^2 Y_n - \alpha_0^2 Y_1 - (\alpha_n^2 - \alpha_0^2)Y_{av} = 0. \tag{101}$$

Combining (100) and (101) with (90) and (91), or (94) and (95), we find that

$$A = [(1 + \delta)(1 + \eta)\ln \rho_0 - 1]Y_{av}, \quad B = (1 + \delta)Y_{av} \tag{102}$$

$$K_1 = \alpha_0^2(Y_{av} - Y_1) + \gamma Y_{av}, \quad K_n = \alpha_n^2(Y_{av} - Y_n) + \gamma Y_{av} \tag{103}$$

where

$$\delta = \frac{\alpha_0 m_0 Y_1 + \alpha_n m_n Y_n}{\sqrt{3}(\alpha_n^2 - \alpha_0^2)Y_{av}} \tag{104}$$

$$\gamma = \alpha_0 \alpha_n \frac{\alpha_0 m_n Y_n + \alpha_n m_0 Y_1}{\sqrt{3}(\alpha_n^2 - \alpha_0^2)Y_{av}} \tag{105}$$

for the friction factor conditions (90) and (91), and

$$\delta = \frac{(\alpha_0 \mu_0 + \alpha_n \mu_n)[1 - (1 + \eta)\ln \rho_0 + J]}{(\alpha_n^2 - \alpha_0^2) + (\alpha_0 \mu_0 + \alpha_n \mu_n)[(1 + \eta)\ln \rho_0 - J]} \tag{106}$$

$$\gamma = \frac{\alpha_0 \alpha_n(\alpha_0 \mu_n + \alpha_n \mu_0)[1 - (1 + \eta)\ln \rho_0 + J]}{(\alpha_n^2 - \alpha_0^2) + (\alpha_0 \mu_0 + \alpha_n \mu_n)[(1 + \eta (\ln \rho_0 - J)]} \tag{107}$$

with the Coulomb friction coefficient conditions (94) and (95).

Summing eqns (89) from $j = 1$ to $j = i - 1$, and using the first of (103), gives

$$K_i = \alpha_0^2(Y_{av} - Y_{av}^{(i)}) + \alpha_i^2(Y_{av}^{(i)} - Y_i) + \gamma Y_{av} \tag{108}$$

where

$$Y_{av}^{(i)} = \frac{1}{\alpha_i^2 - \alpha_0^2} \sum_{j=1}^{i} (\alpha_j^2 - \alpha_{j-1}^2)Y_j \tag{109}$$

is the average yield stress of the first i layers.

The stress field (84)–(86) can now be written explicitly in the form

$$\sigma_r^{(i)} = Y_i - Y_{av} + (1 + \delta)Y_{av}[(1 + \eta)\ln \rho_0 - 2\ln \rho] \tag{110}$$

$$\sigma_\theta = -Y_{av} + (1 + \delta)Y_{av}[(1 + \eta)\ln \rho_0 - 2\ln \rho] \tag{111}$$

$$\tau_{r\theta}^{(i)} = \left[(1 + \delta)\theta - \frac{\alpha_0^2 + \gamma}{\theta}\right]Y_{av} - \frac{\alpha_i^2 - \alpha_0^2}{\theta}Y_{av}^{(i)} + \left(\frac{\alpha_i^2}{\theta} - \theta\right)Y_i. \tag{112}$$

Formally, it remains to find constants U_i which determine the radial velocity profile (87). The velocity continuity conditions at the interfaces imply here the relations

$$U_{i+1} = U_i \quad i = 1, 2, \ldots, n - 1 \tag{113}$$

by which all U_i can be expressed by a single unknown constant U.

The driving stresses (97) and (98) may here be cast into the relations

$$t = (1 + \delta)t_u, \qquad p = (1 + \delta)p_u \qquad (114)$$

where

$$t_u = \frac{1+\eta}{2} Y_{av}\epsilon_0, \qquad p_u = \frac{1-\eta}{2} Y_{av}\epsilon_0 \qquad (115)$$

are the corresponding uniform driving stresses, and

$$\epsilon_0 = 2 \ln \rho_0 \qquad (116)$$

is the total homogeneous strain in axially-symmetric radial flow.

For the case of composite wires, where $\alpha_0 = 0$ and $m_0 = \mu_0 = 0$, we have the simplified relations

$$\gamma = 0, \quad K_i = \alpha_i^2(Y_{av}^{(i)} - Y_i) \quad i = 1, 2, \ldots, n \qquad (117)$$

and

$$\delta = \frac{m_n Y_n}{\sqrt{3}\alpha_n Y_{av}}, \quad \delta = \frac{\mu_n[1 - (1 + \eta) \ln \rho_0 + J]}{\alpha_n + \mu_n[(1 + \eta) \ln \rho_0 - J]} \qquad (118)$$

for the proper expressions of the correction factors. Note that since $K_1 = 0$ the shear stress (86) varies linearly within the core layer.

7. CONCLUDING REMARKS

In the last section we present a brief discussion of the axially-symmetric solution, by way of comparison with the analogous plane-strain results.

Let us begin with the forming processes of a composite tube that consists of a hard core coated with two soft thin layers. Taking $m_0 = m_1 = m$, $Y_1 = Y_n = Y_{coat}$, $Y_{av} = Y_{core}$ and $2(\alpha_n - \alpha_0) = \alpha$ for the effective axially-symmetric die angle, we find from (104) that

$$\delta = \frac{2}{\sqrt{3}} \left(\frac{m}{\alpha}\right) \left(\frac{Y_{coat}}{Y_{core}}\right) \qquad (119)$$

which differs by a factor of $2/\sqrt{3}$ from (54). Expression (119) holds also for a coated wire, with $2\alpha_n = \alpha$, as can be seen from the first of (118).

The relative weight of the shear factors along the walls, for the same Y_i $(i = 1, n)$ Y_{av} and α, is obtained by comparing (104) with (41). It turns out that

$$(m_i)_{\text{plane-strain}} = \frac{\alpha_i}{\alpha_0 + \alpha_n} \left(\frac{4}{\sqrt{3}} m_i\right)_{\text{axially-symmetric}} \quad i = 0, n \qquad (120)$$

which demonstrates why the axially-symmetric tube forming analysis is not valid when $\alpha_0 = 0$; the area of the inner wall vanishes and m_0 becomes meaningless.

A similar relation holds for the Coulomb friction coefficients μ_i. In comparing (106) with (43) we note that ρ_0 in the plane-strain formula is replaced by ρ_0^2 in the axially-symmetric solution. This follows also from a comparison of (96) with (32). With that transformation in mind we find that (106) becomes identical with (43) provided that

$$q = \frac{\alpha_0\mu_0 + \alpha_n\mu_n}{\alpha_n^2 - \alpha_0^2} \qquad (121)$$

replaces, in the axially-symmetric case, the plane-strain definition (55). The two expressions

for q become identical (for the same die angle) if

$$(\mu_i)_{\text{plane-strain}} = \frac{\alpha_i}{\alpha_0 + \alpha_n} (2\mu_i)_{\text{axially-symmetric}} \quad i = 0, n \tag{122}$$

again showing the invalidity of the tube forming solutions for $\alpha_0 = 0$.

A noteworthy point here is that the expressions for q, given by (55) and (121), admit the common structure

$$q = \frac{2\mu_{av}}{\alpha} \tag{123}$$

where the average Coulomb friction coefficient μ_{av} is defined by $\mu_{av} = \frac{1}{2}(\mu_0 + \mu_n)$ in plane-strain, and by $\mu_{av} = (\alpha_0\mu_0 + \alpha_n\mu_n)/(\alpha_0 + \alpha_n)$ in the axially-symmetric case. Note again that the respective die angles are $\alpha = \alpha_n - \alpha_0$ and $\alpha = 2(\alpha_n - \alpha_0)$.

Expressions (43) and (106) can therefore be written in the common formula

$$\delta = \frac{q(1 - J^*)}{1 + qJ^*} \tag{124}$$

where

$$J^* = 1 + \left(\frac{1 + \eta}{2} - \frac{\rho_0}{\rho_0 - 1}\right) \ln \rho_0 \tag{125}$$

in plane-strain, and ρ_0 is replaced by ρ_0^2 in the axially-symmetric flow. Relations (124) and (125) hold also for composite wire forming processes with $\mu_{av} = \mu_n$ and $\alpha = 2\alpha_n$.

The similarity between the two-dimensional and three-dimensional radial flow patterns implies an almost direct correspondence between the properties of the respective solutions. The basic conclusions drawn in Section 4 are therefore valid for the axially-symmetric forming processes as well. In restriction (62), for example, we simply replace ϵ_0 by definition (116). Similarly, constraints (63) are here replaced by

$$\left|(\alpha_i^2 - \alpha_0^2)(Y_{av} - Y_{av}^{(i)}) + (\alpha_0^2\delta - \gamma)Y_{av}\right| \leqslant \alpha_i\tau_0^{(i)} \quad i = 1, 2, \ldots, n - 1 \tag{126}$$

where $\tau_0^{(i)}$ are the allowable shear stresses at the interfaces.

REFERENCES

1. A. G. Atkins and A. S. Weinstein, *Int. J. Mech. Sci.* **12**, 641 (1970).
2. T. Z. Blazynski and S. Townley, *Int. J. Mech. Sci.* **20**, 785 (1978).
3. D. Durban and B. Budiansky, *J. Mech. Phys. Solids* **26**, 303 (1979).
4. D. Durban, *J. Appl. Mech.* **46**, 322 (1979).
5. D. Durban, *J. Appl. Mech.* **47**, 736 (1980).
6. D. Durban, *Int. J. Mech. Sci.* **25**, 27 (1983).
7. A. Nadai, *Z. Phys.* **30**, 106 (1924).
8. R. Hill, *The Mathematical Theory Of Plasticity*, Oxford (1950).
9. R. T. Shield, *J. Mech. Phys. Solids* **3**, 246 (1955).
10. C. Truesdell, *J. Rational Mech. Anal.* **2**, 173 (1953).
11. R. R. Arnold and P. W. Whitton, *Proc. Inst. Mech. Engrs* **173**, 241 (1954).